

## $^2\text{H}$ ENDOR and FTESEEM of the TANOLD Spin Probe in an Amine-Cured Epoxy Matrix<sup>†</sup>

M. D. Pace\*

Code 6120, Naval Research Laboratory, Washington, D.C. 20175-5342

I. M. Brown

McDonnell Douglas Aerospace-East, St. Louis, Missouri 63166

Received June 16, 1993; Revised Manuscript Received December 14, 1993\*

**ABSTRACT:** Fourier transforms of the electron spin echo envelope modulation (FTESEEM) patterns of deuterated TANOLD spin probes (4-hydroxy-2,2,6,6-piperidiny-1-oxy- $d_{17}$ ) in the amine-cured diglycidyl ether of bisphenol A epoxy (DGEBA) at room temperature show two pairs of deuterium lines displaced about the free deuterium frequency (2.2 MHz) which are assigned to the electron-nuclear hyperfine couplings of inequivalent  $-\text{CD}_3$  groups of the nitroxide. Conformational asymmetry of the  $-\text{CD}_3$  groups accounts for the experimentally observed two pairs of spectral lines at room temperature and the disappearance of one pair of lines at 100 K. In this model, it is suggested that two conformational states of the spin probe molecules are thermally populated as the temperature is increased from 100 K to room temperature. Continuous wave electron-nuclear double resonance (ENDOR) spectra support the FTESEEM results. Nuclear quadrupole interactions, as an alternative explanation for the observed splittings, are shown not to fully account for the experimental observations.

### Introduction

Several previously reported studies<sup>1-3</sup> of nitroxide spin probes in amine-cured epoxy resins have been mainly concerned with the behavior of the motional correlation times ( $\tau_c$ ) of the nitroxide at temperatures both above and below the glass transition temperature ( $T_g$ ) of the matrix. The goal of these studies was to use the nitroxide to provide information at a molecular level about static and dynamic environments in the polymer. Above  $T_g$  the  $\tau_c$  values were determined by the free volume content of the polymer as well as the temperature. As a result, these values were found to depend on the pressure, solvent content, spin probe diameter, and the cross-link density of the host polymer matrix. On the other hand, the  $\tau_c$  values below  $T_g$  were remarkably independent of the spin probe diameter and the cross-link density of the host polymer matrix. Above  $T_g$ , the motional narrowing of the EPR line shapes is consistent with end-over-end rotational diffusional motions of the nitroxide, whereas below  $T_g$ , the values of the motional correlation times suggest that the nitroxides are undergoing more restricted motions.

Our original intention in this study was to obtain more information about the restricted motions in the sub- $T_g$  region down to temperatures of 100 K by using advanced electronic spin echo techniques to determine whether dynamic molecular changes of the spin probes could be measured in the amine-cured DGEBA epoxy matrix as a function of temperature between 100 K and room temperature and, if so, to relate these changes to the dynamics of the polymer host. In EPR line shape studies<sup>1,2</sup> that led to an evaluation of the motional correlation times below  $T_g$ , line shift changes of  $\sim 0.01$  mT (0.1 G) could be measured, corresponding to frequency shifts of 280 kHz. On the other hand, in the FTESEEM experiments frequency shifts of only a few kilohertz can be detected. Thus, as this work will show, using FTESEEM techniques, it is possible to measure spectral changes about 2 orders

of magnitude smaller than that detectable from the EPR line shapes. The changes in the FTESEEM spectra that were observed as the temperature was decreased from 180 to 105 K are interpreted in terms of two conformations of the nitroxide spin probe.

Another advantage of the FTESEEM technique is that the microwave pulses excite only selective regions of the inhomogeneously broadened EPR line. Moreover, since this inhomogeneous line shape is determined primarily from anisotropy of the  $g$  value, these selective regions can be chosen to correspond to certain orientations of the nitroxide axes with respect to the external magnetic field. This makes the interpretation of the FTESEEM spectra easier and more reliable. This study will further show that FTESEEM spectra can be used to measure small dipolar hyperfine couplings arising from interactions between the deuterium nuclei located on the four methyl groups and the unpaired spin density at the nitroxyl group of the spin probe molecule 4-hydroxy-2,2,6,6-piperidiny-1-oxy- $d_{17}$  (TANOLD). The hyperfine couplings are related to the distance of the  $^2\text{H}$  nuclei from the  $-\text{N}-\text{O}$  group and to the dihedral angle between the  $\text{N}-\text{C}-\text{CD}_3$  plane and the plane formed by the  $2p_z\pi$  orbital of the nitroxyl group and the  $-\text{N}-\text{O}$  bond axis. This is the familiar dipolar relationship expressed in

$$A_{\text{dipolar}} = g_e g_n \beta_e \beta_n (3 \cos^2 \theta - 1)/r^3 \quad (1)$$

where  $g_e = 2.0023$ ,  $g_n = 0.857$ ,  $\beta_e = 0.92731 \times 10^{-20}$  erg/G,  $\beta_n = 0.505 \times 10^{-23}$  erg/G, and  $r$  is the interatomic distance between  $^{14}\text{N}$  (site of unpaired spin density) and the  $^2\text{H}$  atomic positions.  $\theta$  is the angle between the  $2p_z\pi$  orbital axis direction and the direction of the vector between the  $^{14}\text{N}$  and  $^2\text{H}$  nuclei. The approximations to this expression that were used will be explained under Discussion.

### Experimental Section

Epoxy samples were prepared by incorporating TANOLD (Merck, Sharp and Dohme) in the uncured epoxy resin diglycidyl ether of bisphenol A (DGEBA) (Dow Chemical, DER 332) cured with diethylenetriamine (DETA). The experimental procedure was to first add a measured quantity of TANOLD to the curing agent to ensure solubility in DETA and then to add

<sup>†</sup> Approved for public release export authority (McDonnell Douglas): 22 CFR 125.4 [B] [13].

\* Abstract published in *Advance ACS Abstracts*, February 15, 1994.

the DETA/TANOLD solution to DGEBA such that the final concentration of the spin probe in the cured epoxy equalled 0.1% by weight. The ratio of DETA/DGEBA was in a 1:1 stoichiometric proportion. Curing began instantly upon mixing, but 5–10 min were required before the sample became tacky, allowing time for vortex mixing. Some samples were prepared using DGEBA warmed to 45 °C in an oven to decrease the viscosity before the DETA/TANOLD solution was added. All samples were cured overnight at room temperature and postcured for 15 min at 45 °C to ensure complete curing.

CW EPR spectra were recorded using a Bruker ESP 380 X-band spectrometer. The 0.1% DGEBA/TANOLD sample gives a strong EPR signal. The ESEEM spectra were recorded on a Bruker ESEEM spectrometer at McDonnell Douglas Aerospace. An excitation sequence of three  $\pi/2$  microwave pulses was used, with  $\tau$  (the time between the first and second pulses) = 240 ns, and  $T$  (the time between the second and third pulses) varied. The resulting ESEEM signals were Fourier transformed to give the frequency domain spectra. A Bruker variable-temperature controller was used to collect the temperature-dependent ESEEM spectra. ENDOR spectra were recorded at the Naval Research Laboratory using a Bruker ER 200 spectrometer with ENDOR accessory and Varian temperature controller. Identical DGEBA/TANOLD samples were used in both the ESEEM and the ENDOR studies.

EPR simulations were carried out using a personal computer having a 486 processor or a VAX computer. The time-domain ESEEM simulations were Fourier transformed and manipulated using *Mathematica 2.0* software. The FTESEEM spectra and molecular conformations of the  $-\text{CD}_3$  groups were modeled by using a computer code written specifically for this study.<sup>4</sup>

## Results

**ESEEM Spectra.** The ESEEM experiment, which originally evolved from the work of Rowan, Hahn and Mims, has been previously described.<sup>5–7</sup> ESEEM modulation patterns are recorded and displayed as the time-varying decay signals of the three-pulse echo envelope modulated by beat frequencies due to the hyperfine couplings. The three pulse echo envelope (in which time  $\tau$  is constant and time  $T$  is varied) produces an echo spectrum which is free of sum and difference frequencies that are present in a two-pulse echo envelope. Below  $T_g$  of the amine-cured DGEBA epoxy matrix, the EPR lines are inhomogeneously broadened and the spectral diffusion rates are slow enough to allow the line to be selectively excited by the microwave pulses. This provides an advantage in studying randomly ordered spin systems such as TANOLD, because the microwave pulses can be applied in such a way as to excite only spin probes which have certain orientations with respect to the magnetic field.

The TANOLD absorption line shape shown in Figure 1 illustrates how in the rigid limit the selective orientations of the spin probe depend on the  $m_I(^{14}\text{N})$  values. Figure 1a shows a CW EPR spectrum of a typical nitroxide spin probe randomly oriented in a rigid matrix. In this rigid limit the observed EPR spectrum is the sum of the EPR spectra for all orientations of the spin probe molecules with respect to the external magnetic field direction ( $B_0$ ). The outer lines of the CW DGEBA/TANOLD EPR spectrum therefore correspond to the absorptions of those spin probe molecules which have the major axes ( $Z$ -axes) of their  $^{14}\text{N}$   $2p_z\pi$  orbitals (the site where the unpaired electron is localized) aligned parallel to  $B_0$ . EPR spectra of the "parallel" (those molecules with the  $2p_z$  orbital parallel to  $B_0$ ) and "perpendicular" (those molecules with the  $2p_z$  orbital perpendicular to  $B_0$ ) orientations are shown in Figure 1b,c. When the magnetic resonance field is set to correspond to the resonance frequency of either extremum turning point of the CW spectrum, an FTESEEM spectrum of only those molecules in the parallel orientations is selectively recorded. This experiment has

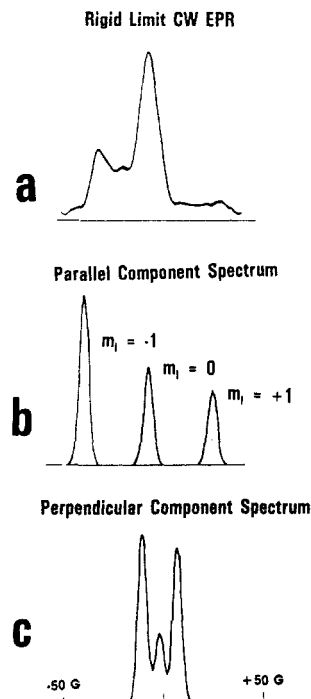


**Figure 1.** (a) Experimental "rigid limit" absorption CW x-band EPR spectrum for a typical nitroxide spin label having approximate  $^{14}\text{N}$  hfc values of  $A_{zz} = 32$  G,  $A_{xx} = A_{yy} \approx 8$  G, and  $g_{xx} = 2.008$ ,  $g_{yy} = 2.006$ , and  $g_{zz} = 2.002$ . (Axes  $X$ ,  $Y$ , and  $Z$  are with respect to the spin probe molecule with  $X$  along the  $-\text{N}-\text{O}^{\bullet}$  bond,  $Z$  along the nitrogen  $2p_z\pi$  axis direction, and  $Y$  orthogonal to both  $X$  and  $Z$ .) (b) Calculated parallel component ( $A_{zz}$  and  $g_{zz}$ ) of the nitroxide CW EPR spectrum. The  $m_I(^{14}\text{N}) = -1$  component corresponds to the resonance position which was used to record the FTESEEM deuterated methyl group spectra in this study. (c) Calculated perpendicular component ( $A_{xx}$ ,  $A_{yy}$  and  $g_{xx}$ ,  $g_{yy}$ ) of the CW rigid limit EPR spectrum. Although this component is due to singular (perpendicular) orientations of the magnetic field, this component falls at the center of the spectrum and is overlapped with other orientational components.

been successfully demonstrated by ENDOR experiments of nitroxides in frozen glasses.<sup>8</sup> When the resonance magnetic field is moved toward the center of the CW EPR spectrum, the response corresponds to that from several overlapping orientations of spin probes in the DGEBA system.

In our experiments, the magnetic resonance field was set at the low field ( $m_I = -1$  transition) of the EPR spectrum of the DGEBA/TANOLD sample and the three-pulse ESEEM patterns were recorded. Figure 2a shows the echo envelope modulation produced by the deuterium nuclei in TANOLD at room temperature, and Figure 2b is the corresponding Fourier transform (FTESEEM) spectrum. This FTESEEM spectrum exhibits four resolved peaks which we refer to as the "inner" pair (2.13 and 2.34 MHz) and the "outer" pair (1.98 and 2.46 MHz) of lines. The splittings associated with these inner and outer pairs of lines are denoted I and O, respectively. These lines are centered at the free deuterium frequency of 2.2 MHz. Also shown in Figure 2c is an ENDOR spectrum of the DGEBA/TANOLD sample recorded at 240 K.

Figure 3 shows the CW derivative of EPR spectrum and several FTESEEM spectra of the amine-cured DGEBA/TANOLD sample recorded for different magnetic field values and at different temperatures between 100 K and room temperature. As can be seen from Figure 3 with  $B_0$  set at the low-field extremum value (the  $m_I(^{14}\text{N}) = -1$  parallel component), the FTESEEM spectrum at 100 K exhibits two peaks centered at the free deuterium frequency (2.2 MHz) and separated by a splitting of 500 kHz. As the temperature is increased, a second pair of peaks

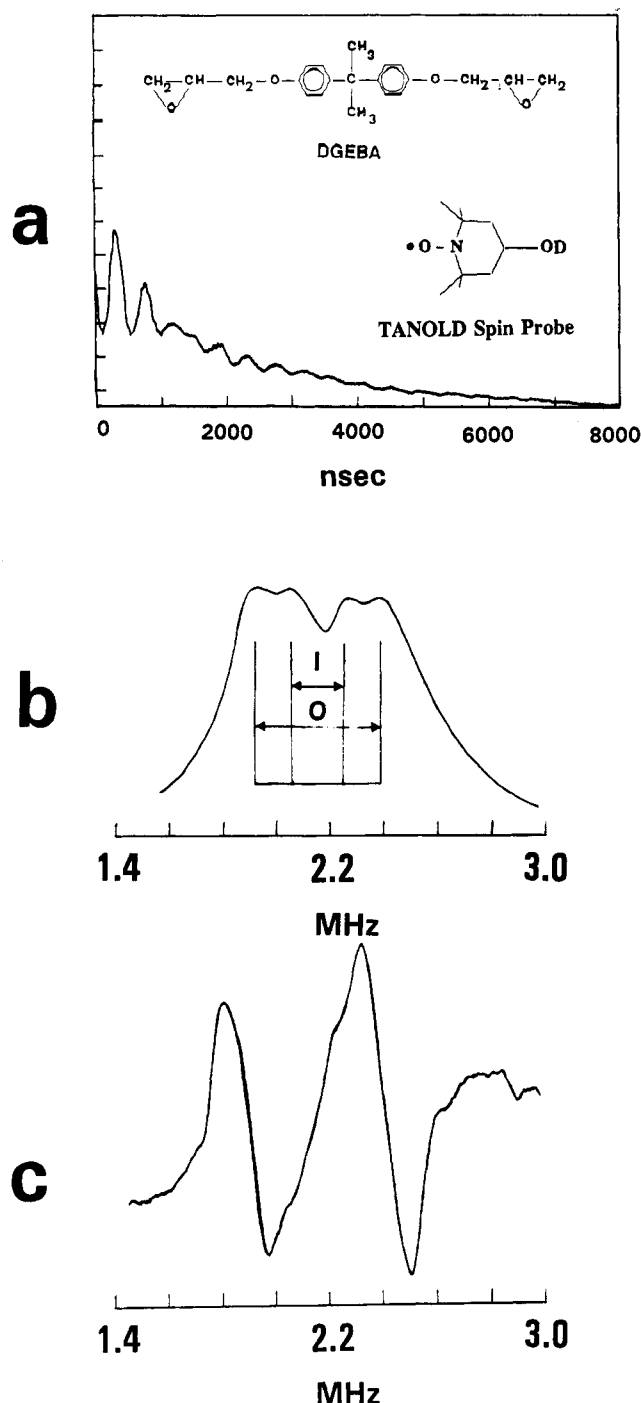


**Figure 2.** (a) Room temperature ESEEM spectrum recorded for the DGEBA/TANOLD sample with  $B_0$  set at the  $m_I(^{14}\text{N}) = -1$  line of the CW spectrum. (b) Fourier transform (FTESEEM) deuterium spectrum of Figure 1a. The spectrum shows two pairs of lines referred to as the inner pair (215-kHz splitting, denoted I) and the outer pair (465-kHz splitting, denoted O). (c) ENDOR spectrum displayed as a first-derivative line shape of DGEBA/TANOLD recorded at  $-30^\circ\text{C}$  ( $\sim 240\text{ K}$ ) with the magnetic field set at the  $m_I = -1$  line of the CW EPR spectrum.

(the inner pair) appears at 135 K between the outer peaks and increases in intensity at higher temperatures until at 300 K the four-line spectrum shown in Figure 2b is observed. The appearance and disappearance of the inner pair of peaks is completely reversible with temperature and is only clearly resolved at the low- and high-field extrema magnetic field values corresponding to the  $m_I(^{14}\text{N}) = \pm 1$  parallel components of the EPR spectrum.

A plot of the temperature dependence of the hyperfine splittings for the inner and outer pairs is given in Figure 4. The separation between the temperature-dependent outer set of FTESEEM peaks first increases from 500 kHz at 100 K to a maximum of 530 kHz at 180 K and then

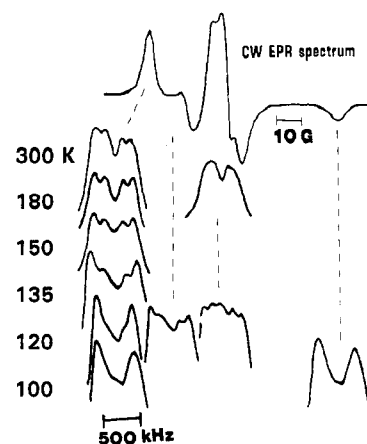


**Figure 3.** Different FTESEEM deuterium spectra recorded as a function of temperature between 100 K and room temperature (300 K) and as a function of magnetic resonance field position in the CW EPR spectrum. The spectral changes with resonance position are assigned to variations of probe orientational order. The temperature-dependent changes are assigned to differing ring conformations of the spin probes in the solid DGEBA epoxy.

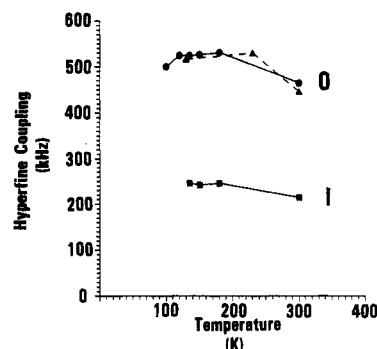


**Figure 4.** Plot of the experimental deuterium hyperfine couplings vs temperature for the outer (O) hyperfine coupling measured by ESEEM (●) and ENDOR (▲) and for the inner hyperfine coupling (I) measured by ESEEM (■).

**Table 1. Temperature-Dependent Hyperfine Splittings<sup>a</sup>**

temp (K)	O (kHz)	I (kHz)	temp (K)	O (kHz)	I (kHz)
300	465	215	135	524	246
180	531	246	120	524	
150	526	242	100	500	

<sup>a</sup> I and O refer to the inner and outer splittings as shown in Figure 2b.

decreases to 465 kHz at room temperature. The inner set of peaks is not observed in the FTESEEM spectra at 100 K but has a separation of 246 kHz at 135 K (where first measurable) and a separation of 215 kHz at room temperature. The hyperfine splittings are listed in Table 1.

**ENDOR Spectra.** The splitting values were confirmed for the outer peaks by measuring CW ENDOR spectra of DGEBA/TANOLD sample. The  $^2\text{H}$  ENDOR spectra recorded at 140, 250, and 300 K for the  $m_I(^{14}\text{N}) = -1$  parallel component field resonance position show splitting values (Figure 4) similar to those of the FTESEEM spectra for the outer pair of lines (O). As in the FTESEEM spectra, the splitting of the outer peaks in the ENDOR spectra is observed to decrease from 530 (180 K) to 465 kHz at room temperature. The ENDOR spectrum (not shown) of the center CW EPR resonance position, where  $m_I(^{14}\text{N}) = 0$ , reveals a maximum coupling of 460 kHz at 180 K. This is consistent with the FTESEEM spectrum of the center peak at 180 K, which is 460 kHz. The inner peaks are not as well-resolved in the derivative ENDOR spectra but can be detected in second-derivative displays of the ENDOR signals. This may indicate that the CW ENDOR line

widths are broader than the FTESEEM spectral line widths, which is not too surprising since the mechanisms for the two types of ENDOR are different.

## Discussion

There are two possible explanations for the room temperature FTESEEM spectrum shown in Figure 3. The two pairs of lines are either the result of inequivalent methyl deuterium hyperfine couplings or the methyl deuterium hyperfine couplings are all equivalent and the additional splitting is due to a quadrupole interaction. For example, when the magnetic field is along the *Z* principal axis, the observed ENDOR frequency ( $\nu$ ) is given by

$$\nu = |\nu_D \pm A_{zz}/2 + Q_{zz}| \quad (2)$$

where  $\nu_D$  is the deuterium Larmor frequency and  $A_{zz}$  and  $Q_{zz}$  are the *z* components of the principal axis of the hyperfine and quadrupole tensor interactions, respectively. However, the temperature dependence of the FTESEEM spectra shown in Figure 4 provides strong evidence that the methyl groups are inequivalent.

**Quadrupole Couplings.** The following analysis presents evidence that quadrupole couplings do not account for the observed FTESEEM spectra. The effects of quadrupole couplings, isotropic hyperfine couplings (hfc), and anisotropic dipolar hfc on three-pulse FTESEEM spectra were calculated by using a computer program which was written using the equations described by Narayana and Kevan<sup>9</sup> and based on the original equations of Mims.<sup>10</sup> The equations in ref 9 describe a model for interaction of a trapped electron with nuclei in a surrounding sphere of radius *r* in a disordered solid. ESEEM patterns were computed for zero isotropic hyperfine coupling, the dipolar coupling was determined by the radius of the nuclear sphere, and the quadrupole coupling varied. Integrations over all angles of orientation give the ESEEM pattern expected for randomly ordered electron-nuclear interactions in a solid. In our computer program we have allowed for integration over any solid angle between 0 and  $\pi$  to take into account varying degrees of disorder and we have allowed for more than one *r* value. Our interpretation of this model differs from ref 9 in that we consider that the splittings are due to intramolecular interactions rather than intermolecular superhyperfine interactions. This is justified since we are dealing with a nitroxide radical where the closest nuclei to the unpaired electron site are intramolecular.

Figure 5 shows FTESEEM spectra simulated for varying values of the deuterium quadrupole coupling up to a maximum value of 225 kHz, which would be the maximum value if the applied magnetic field was exactly aligned along the C-D bond axis. There are several marked inconsistencies of the calculated spectra with the observed data: (i) First, we expect a quadrupole splitting to be dynamically averaged in such a way that a four-line FTESEEM spectrum could reduce to a two-line spectrum at higher temperatures. If a quadrupolar coupling is assigned, then at 100 K the two observed spectral lines in Figure 4 would correspond to averages of frequencies of the FTESEEM lines observed above 135 K. In fact, the observed separation between the outer lines is actually greater at 100 K (500 kHz) than at room temperature (465 K). Also, our results in Figure 4 show that a different temperature dependence is observed in that two lines change to four lines at higher temperatures—a behavior that cannot be explained by averaging of the quadrupolar interaction. (ii) Second, the calculation predicts that for high spin probe disorder, such as a resonance position

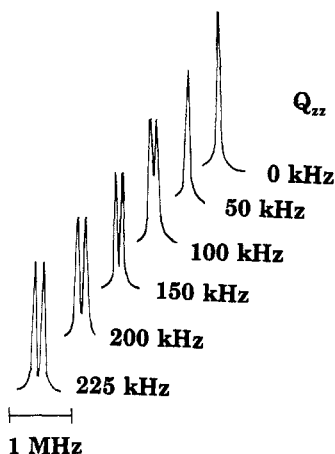


**Figure 5.** Simulated FTESEEM deuterium spectra using the program based on ref 9 with varying quadrupole couplings for an average of probe orientations within a solid angle of  $10^\circ$  to the *p*-orbital axis described in Figure 6. The quadrupole splitting ( $Q_{zz}$ ) is equal to  $2\Delta_0$  in the notation of ref 9 and assigned a maximum value of 225 kHz in the calculations. The maximum possible  $^2\text{H}$  quadrupole coupling measured from the calculated FTESEEM spectra is 120 kHz, giving a spectral splitting less than the difference of 150 kHz between the splittings I and O of Figure 4 at 185 K.

near the center of the CW spectrum, the deuterium quadrupole couplings average to small values, so that the quadrupole splittings would be line broadened. This does not agree with the experimental ESEEM spectra because inner peaks are resolvable at 120 K for the magnetic field set near the center of the CW EPR spectrum, inconsistent with this calculation. (iii) Third, quadrupole interaction values of 120 kHz for (C4D<sub>3</sub>, C4'D<sub>3</sub>) and 70 kHz for (C5D<sub>3</sub>, C5'D<sub>3</sub>), the deuterated methyl group pairs, are calculated for a geometry having the crystal structure conformation (Figure 6). The observed separation between the inner and outer pairs of lines in the experimental spectrum (150 kHz) at room temperature is greater than the maximum value predicted (120 kHz) for the deuterium quadrupole splitting.

**Methyl Group Conformations above 135 K.** On the basis of evidence from ENDOR results and computer-simulated ESEEM time domain and FTESEEM frequency domain spectra, we can account for the two pairs of splittings in Figures 2 and 3, observed above 135 K, by two unequal electron-deuterium dipolar hyperfine couplings.<sup>11,12</sup> The separation between each pair, I and O, corresponds to two different deuterium hyperfine couplings with frequencies such that

$$\nu = \nu_D \pm A_D/2 \quad (3)$$

These deuterium couplings are assigned to the two pairs of asymmetric deuterated methyl groups on the TANOLD spin probe molecule.

We will show using a computer model that conformational changes of the spin probes can account for both the observed FTESEEM and ENDOR spectra. To simplify the calculation, the model uses bond distances and bond angles determined by neutron diffraction.<sup>13</sup> Figure 6 gives a diagram of the molecular model. The spin probe molecular plane is taken as the C3-N-C3' plane (atomic numbering system used is that in ref 13). The O-N-C3' plane is inclined  $12^\circ$  to the N-C3-C2 plane; however, for this calculation unit unpaired spin density is assumed to lie at the nitrogen nucleus (i.e., no unpaired spin density on oxygen). (We found that dipolar calculations with the unpaired  $\pi$ -electron spin density equally distributed on the oxygen and nitrogen atoms of the nitroxyl group lead

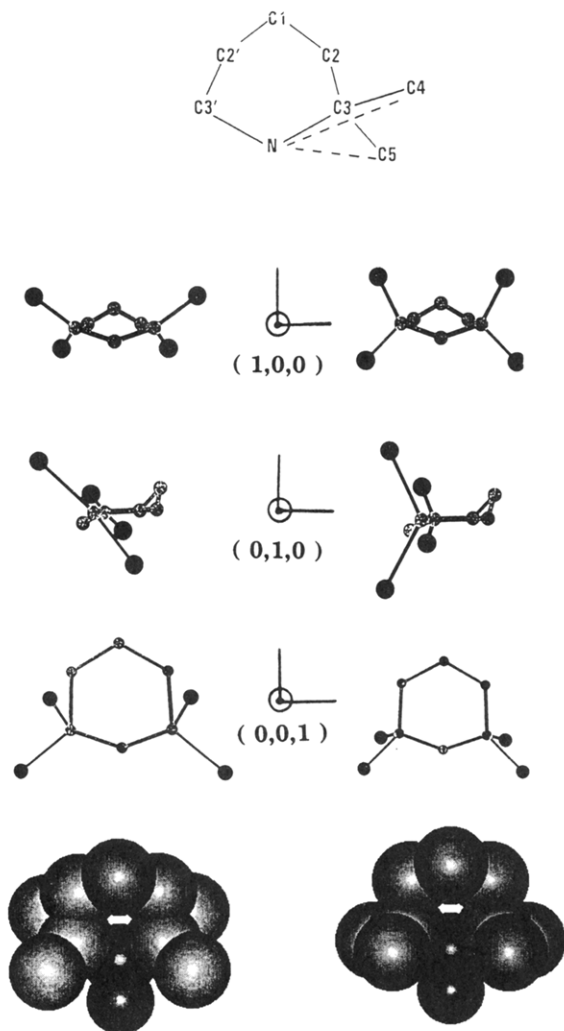


**Figure 6.** (Top) Atomic labeling system; view along the (0.707,0,0.707) direction of the unit cell frame of ref 13 showing an individual spin probe molecule. For clarity, all deuterium nuclei, the -OD group, and oxygen nucleus are not shown, C4, C4' and C5, C5' effective methyl group positions are indicated by the black circles. The dashed lines indicate the interatomic directions and distances N→C4 and N→C5 used in the dipolar calculation. The p orbital is along a direction (0.558,0,0.83) in this model. The two conformations which are consistent with the FTESEEM spectra are shown. The left column gives a spin probe conformation (conformation I) which corresponds to hyperfine coupling constants I and O in Figure 4. The right column gives identical views for a spin probe conformation (conformation II) corresponding to hyperfine coupling O in Figure 4 below 135 K and is identical to the crystal structure spin probe conformation of ref 13. Reading top to bottom, views are shown along the (1,0,0) unit cell direction (top), along the (0,1,0) unit cell direction (middle), and along the (0,0,1) unit cell direction (bottom). (Bottom) Space filling models viewed perpendicular to the C3-N-C3' plane for conformations I and II with the oxygen nucleus included.

to the same general conclusions, regarding the nitroxide conformations, as the simplified calculation with the total spin density located at the nitrogen atomic position. Calculations based on molecular orbital theory would be needed for a more accurate coupling analysis.) Therefore, the oxygen position is not shown in Figure 6 except in the space filling models, and the -OD group is omitted for clarity. The methyl groups are rotating rapidly at the temperatures studied, so to simplify the dipolar calculations, a single coordinate was used to represent an average position representing the three deuterium nuclei on each rotating methyl group. The average deuterium coordinates of -C4D<sub>3</sub> and -C5D<sub>3</sub> were assigned the same coordinates as the carbon nuclei, namely, C4 and C5, respectively (or

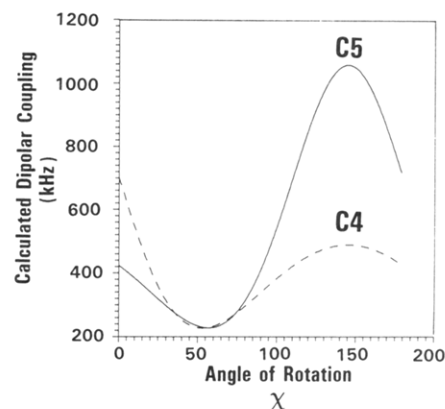


**Figure 7.** Plot of the calculated dipolar hyperfine coupling constants vs the angle of rotation  $\chi$  of the plane C4-C3-C5 about the bisector of the angle C4-C3-C5 in the molecular model of Figure 6. For  $\chi \approx 44^\circ$ , the dipolar couplings of the C4 and C5 positions are both at a minimum and approximately equal to the splitting of I in Figure 2. See text for explanation of the model conformations.

**Table 2. Molecular Coordinates of Spin Probe Model**

	X	Y	Z
Ring Coordinates <sup>a</sup>			
N	0.391	0.0	-0.171
O2	0.513	0.0	-0.212
C3	0.334	0.133	-0.132
C2	0.183	0.123	-0.116
C1	0.139	0.0	-0.039
Methyl Group Conformations			
conformation I			
C4	0.421	0.219	-0.470
C5	0.245	0.219	-0.218
conformation II			
C4	0.400	0.178	-0.001
C5	0.366	0.232	-0.245

<sup>a</sup> Ring coordinates given in nm ( $10^{-9}$  m) based on ref 13. C3', C2', C4', C5' coordinates equal to (x,-y,z) of the respective unprimed coordinated.

C4' and C5' for symmetrically related atoms).<sup>14</sup> Different conformations were computer modeled by rotating the C4 and C5 coordinates (i.e., the C3-C4 and C3-C5 bond directions) about the bisector of angle C4-C3-C5. This approximates geometric changes of C4 and C5 relative to <sup>14</sup>N which might occur if the molecule changes conformations. For each angle,<sup>15</sup> the dipolar hyperfine couplings between the effective deuterium positions C4 (and C4') and C5 (and C5') and the <sup>14</sup>N atomic coordinate were calculated. The calculated dipolar couplings versus the angle of rotation ( $\chi$ ) are shown in Figure 7. For  $\chi = 40-50^\circ$  both C5 and C4 positions give a dipolar coupling of ca. 250 kHz, which is approximately the value of the inner pair of lines at 180 K (246 kHz). Refinement of the calculation gives good agreement with this experimental value for  $\chi = 44^\circ$  (230 kHz). Using  $\chi = 44^\circ$ , we can therefore calculate the molecular coordinates within the unit cell reference frame of ref 13 or the C4 and C5 (and C4' and C5') positions predicted by this model. These X, Y, and Z coordinates are, for C4, (0.421 nm, 0.219 nm, -0.470 nm) and, for C5, (0.245 nm, 0.219 nm, -0.218 nm). Table 2 gives complete model coordinates. We use the unit cell reference frame for convenience and limit our analysis to the FTESEEM and ENDOR spectra recorded at the  $m_I = -1$  line of the CW EPR spectrum of Figure 3. These coordinates correspond to a spin probe conformation as shown in Figure 6 for conformation I. Three views are given for molecule 1 of the unit cell: the view along (1,0,0), (0,1,0), and (0,0,1) directions. The acute angle between the p-orbital axis and the N→C4 vector is  $61^\circ$ , and the

N→C4 internuclear distance is 0.254 nm. The angle between the p-orbital axis and the N→C5 direction is 64°, and the N→C5 distance is 0.267 nm.

**Methyl Group Conformations below 135 K.** Figure 6 also predicts a conformation consistent with the deuterium hyperfine coupling constants observed below 135 K. For  $\chi = 20^\circ$  or  $95^\circ$  a hyperfine coupling constant of ca. 530 kHz is predicted for C5 (C4 also changes but does not equal values of either 240- or 530-kHz couplings). The  $\chi = 20^\circ$  conformation is unrealistic because of steric hindrance with the ring nuclei. However, the  $\chi = 95^\circ$  conformation is very similar to the crystal structure conformation of ref 13. Therefore, we consider the crystal structure conformation as that predicted by our model and given as conformation II in Figure 6. Below 135 K the disappearance of the inner pair of lines can be accounted for by the crystal structure conformation in which both methyl groups lie in a plane (C4–N–C5) which has a dihedral angle of  $75^\circ$  to the C3–N–C3' plane. In this conformation, the N→C5 distance is 0.244 nm and the corresponding angle between N→C5 direction and the  $2p_z$  orbital direction is  $72^\circ$ . This corresponds to a hyperfine coupling constant matching that observed experimentally at 125 K (530 kHz). For the C4 position, a very small dipolar coupling ( $>10$  kHz) occurs in this conformation because the N→C4 distance is 0.246 nm and the angle between the N→C4 direction and the  $2p_z$  orbital direction (taken as the perpendicular to the C3–N–C3' plane of our model) is  $55^\circ$ .<sup>16</sup> This effect does not show up in Figure 7 because the simple model does not exactly mimic the crystal structure conformation.

Our mechanism for populating the second conformational state of TANOLD above 135 K is suggested to be a thermally induced conformational change. This would be consistent with the increase in intensity of the inner  $^2\text{H}$  lines in Figure 3 from 135 K to room temperature since at higher temperature more probes would thermally populate this conformational state. Reduction in the coupling constants, as shown in Figure 4, from 180 K to room temperature is probably the result of dynamic motional averaging produced by the restricted motions described previously.<sup>1,2</sup>

Although our previous sub- $T_g$  studies<sup>1</sup> established that the nitroxide motions were restricted, little was learned about the polymer dynamics, the coupling of these motions to the intramolecular nitroxide motions, or the packing of the polymer around the nitroxide. On the other hand, our EPR studies clearly showed that the polymer dynamics and the polymer packing allowed, even if they did not cause, such restricted motions to take place. In this paper our EPR studies again do not indicate any details about the polymer dynamics or the polymer packing, but the results clearly indicate that both allow molecular conformational changes to take place. Thus, our studies both here and previously<sup>1</sup> have established two main features of nitroxide spin probe behavior in host polymers below  $T_g$ , viz., restricted nitroxide motions and conformational changes. In any future sub- $T_g$  studies that may throw light on the polymer dynamics or the polymer packing, neither the restricted motions nor the possible conformational changes can be ignored.

We note that the two conformations shown in Figure 6 are not necessarily unique fits to the dipolar coupling data but are the best predictions of our simple model approach. Semiempirical molecular orbital calculations would be needed to refine the model conformations.

## Summary

It was demonstrated that subtle conformational changes of the spin probe TANOLD dissolved in a rigid epoxy

matrix can be detected from FTESEEM and CW ENDOR spectra even when these changes are not detectable from CW EPR spectra. A molecular model of TANOLD based on the deuterated methyl group dipolar hyperfine interactions obtained from the FTESEEM spectra shows that a spin probe conformation (conformation II, Figure 6) corresponds to a hyperfine splitting denoted O in Figure 4 and is similar to the crystal structure conformation. A second spin probe conformation which corresponds to a hyperfine splitting, denoted I in Figure 4 (conformation I, Figure 6), has methyl groups rotated by ca.  $44^\circ$  from their original positions and is suggested to be thermally populated above 135 K. This accounts for the appearance of two additional FTESEEM spectral lines and hence the nonequivalence of the two methyl groups above 135 K. In addition, CW ENDOR spectra recorded between 140 and 300 K exhibit splittings similar to those measured by FTESEEM for the hyperfine coupling constant denoted O in Figure 4. Quadrupole couplings do not account for the observed magnitudes of changes in the splittings of the FTESEEM spectra. An ENDOR measurement, made subsequent to this research, of proton hyperfine couplings in a spin-labeled DGEBA polymer supports our methyl deuterium hyperfine coupling assignments.

**Acknowledgment.** The Office of Naval Research is acknowledged for sponsoring M.D.P. on the Edison Advanced Research Program while at McDonnell Douglas. This work was performed in part under the McDonnell Douglas Independent Research and Development Program. Dr. Hans van Willigen of the University of Massachusetts, Boston, is acknowledged for his helpful suggestions. Dr. A. N. Garroway of the Naval Research Laboratory is acknowledged for discussion of motional averaging effects on nuclear magnetic resonance lines.

## References and Notes

- (1) Sandreczki, T. C.; Brown, I. M. *Macromolecules* **1988**, *21*, 504.
- (2) Brown, I. M.; Sandreczki, T. C. *Macromolecules* **1985**, *18*, 1789.
- (3) Brown, I. M.; Sandreczki, T. C. *Macromolecules* **1985**, *18*, 2702.
- (4) The spin echo program used for our simulations is based on a program provided by Dr. L. Kevan, University of Houston, Houston, TX.
- (5) Rowan, L. G.; Hahn, E. L.; Mims, W. B. *Phys. Rev.* **1965**, *A137*, 61.
- (6) Mims, W. B. *Phys. Rev.* **1972**, *B5*, 2409.
- (7) Mims, W. B. *Phys. Rev.* **1972**, *B6*, 3543.
- (8) Mustafi, D.; Joela, H.; Makinen, M. W. *J. Magn. Reson.* **1991**, *91*, 497.
- (9) Narayana, P. A.; Kevan, L. *J. Magn. Reson.* **1979**, *26*, 437.
- (10) Mims, W. B. *Electron Paramagnetic Resonance*; Geshwind, S., Ed.; Plenum: New York, 1972.
- (11) Isotropic hyperfine couplings of the deuterium nuclei in this spin probe would be extremely small because the TANOLD molecule is unconjugated and the deuterium nuclei are separated from the nitroxyl group by a distance of three atomic nuclei. See ref 12 for a recent example of dipolar hyperfine couplings of methyl group protons of a nitroxide.
- (12) Pace, M. D.; Christidis, T. C.; Hyde, J. S. *J. Magn. Reson.* **1993**, *102*, 101.
- (13) Berliner, L. J. *Acta Crystallogr.* **1969**, *B26*, 1198.
- (14) C4' and C5' are related to C4 and C5 by a mirror plane. See ref 13.
- (15) In the model, the angle of rotation of the C4–C3–C5 plane about the bisector of the C4–C3–C5 angle is denoted  $\chi$ . For  $\chi = 0$  or  $\pi$ , C4 and C5 lie within the plane defined by C3–N–C3', with  $\chi$  measured in steps of  $1^\circ$  ( $1^\circ = \pi/180$  rad) from 0 to  $\pi$ . Note that the C4–C3–C5 angle is held constant at  $110^\circ$  in this model.
- (16) The deuterium hyperfine coupling constant vanishes because for this orientation the angle between the N→C4 direction and the p-orbital axis is ca.  $55^\circ$ . The dipolar hyperfine coupling constant, therefore, approaches zero because  $3 \cos^2 \theta \approx 1$  in eq 1. At this same conformation, the angle between the N→C5 direction and the p-orbital axis is  $72^\circ$ , giving a hyperfine coupling constant of ca. 540 kHz.